Oxide based quasiperiodic photonic crystal

Submitted By

Bhavani Prasad Behera

School of Physical Sciences

National Institute of Science, Education and Research (NISER), Bhubaneswar

Under the Guidance of

Dr. Pratap Kumar Sahoo

Associate Professor

School of Physical Sciences

National Institute of Science, Education and Research (NISER), Bhubaneswar

ACKNOWLEDGEMENT

I owe my deepest gratitude to Dr. Pratap Kumar Sahoo whose guidance and expertise have been invaluable in steering us towards success. I also extend my gratitude to my lab mates for their help and feedback.

Finally, I would like to thank my family and friends for their continuous support and encouragement throughout the project.

ABSTRACT

Photonic crystals represent a remarkable advancement in the field of optical materials, offering unprecedented control over light propagation through the manipulation of photonic band gaps. Their unique ability to confine and direct light has significant implications for various applications, ranging from telecommunications and sensing to energy-efficient lighting and imaging technologies. In this project, we create a 1-d quasiperiodic photonic crystal out of ZnO and SiO_2, and study its various transmission spectra, along with other characteristics. We also discuss numerical methods that will help us to calculate band structures and transmission characteristics of photonic crystals.

TABLE OF CONTENTS

1 Introduction

Controlling light propagation in materials has become a rapidly growing area of research. Optical waveguides, for instance, are an incredible technique that has revolutionized communications technology. Photonic crystals offer us a way to control light propagation, allowing certain frequencies to pass through while forbidding others. It is analogous to the electronic states in crystals, where states with certain frequencies are allowed to propagate in certain directions. At the same time, other frequencies might not be able to propagate through the crystal, resulting in a bandgap. Photonic crystals can be considered an optical analogue of crystals, where the periodic potential is replaced by the periodic variation in the dielectric constant inside the medium. The photonic crystals thus give us a way to control and manipulate light propagation. An n-d photonic crystal has a periodically varying dielectric potential along n directions (n = 1, 2, 3).

The frequencies that are not able to transmit through the crystal constitute the photonic band gap (PBG). If, for some frequency range, a photonic crystal prohibits the propagation of electromagnetic waves of any polarization traveling in any direction from any source, we say that the crystal has a complete photonic band gap. A crystal with a complete band gap will be an omnidirectional reflector. Photonic crystals have found applications in a wide range of fields, including telecommunications, sensing, imaging, and even medical diagnostics. By tailoring their structural properties, researchers can engineer devices that exhibit extraordinary optical characteristics, such as superlenses that overcome the diffraction limit or filters with unprecedented selectivity.

The periodicity of these crystals is comparable to the wavelength of light. The varying optical density causes the light to interfere with each other coherently. The range of frequencies that undergo destructive interference cannot transmit through the crystal. This range of frequencies forms the photonic band gap. Light waves within these frequencies are totally reflected back.

The mathematical modeling of these crystals involves solving Maxwell's equations with periodic permittivity. The equation is second order differential equation whose eigenvalues are the frequencies. The dispersion relation obtained from this equation gives an idea about the band gap.

The main characterizations of such crystals are optical characterizations like reflectivity and transmission spectrum measurements. These characteristics determine how the sample interacts with light and how can we tune the properties of the material to get desired results.

2 Theoretical Background and Numerical Methods

2.1 Maxwell's equations

Macroscopic Maxwell's equations describe the behavior of electric and magnetic fields inside a medium. They are given by the following equations,

$$\begin{aligned} \nabla.\mathbf{D}(\mathbf{r},t) &= \rho \\ \nabla.\mathbf{B}(\mathbf{r},t) &= 0 \\ \nabla\times\mathbf{E}(\mathbf{r},t) &= -\frac{\partial\mathbf{B}(\mathbf{r},t)}{\partial t} \\ \nabla\times\mathbf{H}(\mathbf{r},t) &= \mathbf{J}(\mathbf{r},t)+\frac{\partial\mathbf{D}(\mathbf{r},t)}{\partial t} \end{aligned} \tag{1}$$

We assume that our medium is lossless and there are no free charges or currents or light sources. Thus, we can set $\rho = 0$ and $J = 0$. The electric displacement (D) and the magnetic field strength can be written as,

$$\begin{aligned} \mathbf{D}(\mathbf{r},t) &= \epsilon_0\epsilon(r)\mathbf{E}(\mathbf{r},t) \\ \mathbf{B}(\mathbf{r},t) &= \mu_0\mu(r)\mathbf{H}(\mathbf{r},t) \end{aligned} \tag{2}$$

We have assumed that the electric and magnetic fields are not strong enough to include the higher-order terms in the above equations. We further assume that the dielectric constant is positive and real and that the relative permeability of the medium is nearly equal to one. With all these assumptions, the equations become,

$$\begin{aligned} \nabla.[\epsilon(\mathbf{r})\mathbf{E}(\mathbf{r},t)] &= 0 \\ \nabla.\mathbf{H}(\mathbf{r},t) &= 0 \\ \nabla\times\mathbf{E}(\mathbf{r},t) &= -\mu_0\frac{\partial\mathbf{H}(\mathbf{r},t)}{\partial t} \\ \nabla\times\mathbf{H}(\mathbf{r},t) &= \epsilon_0\epsilon(\mathbf{r},t)\frac{\partial\mathbf{E}(\mathbf{r},t)}{\partial t} \end{aligned} \tag{3}$$

To obtain the wave equation in terms of the electric field, we can take the curl of the third sub-equation of equation (2.3) and substitute the value of the curl of the magnetic field from sub-equation 2. The resulting wave equation is,

$$\nabla\times[\nabla\times\mathbf{E}(\mathbf{r},t)] = -\frac{\epsilon(r)}{c^2}\frac{\partial^2\mathbf{E}(\mathbf{r},t)}{\partial t^2} \tag{4}$$

The wave equation can be written in terms of the magnetic field in a similar manner,

$$\nabla\times[\frac{1}{\epsilon(r)}\nabla\times\mathbf{H}(\mathbf{r},t)] = -\frac{1}{c^2}\frac{\partial^2\mathbf{H}(\mathbf{r},t)}{\partial t^2} \tag{5}$$

We seek the solutions of the form,

$$\begin{aligned} \mathbf{E}(\mathbf{r},t) &= \mathbf{E}(\mathbf{r})e^{-i\omega t} \\ \mathbf{H}(\mathbf{r},t) &= \mathbf{H}(\mathbf{r})e^{-i\omega t} \end{aligned} \tag{6}$$

where ω is the eigen-angular frequency, and $\mathbf{E}(\mathbf{r})$ and $\mathbf{H}(\mathbf{r})$ are the eigenfunctions of the wave functions. Thus we get the following eigenvalue equations,

$$\begin{aligned} \mathcal{L}_E\mathbf{E}(\mathbf{r}) &= \frac{1}{\epsilon}(r)\nabla\times[\nabla\times\mathbf{E}(\mathbf{r})] = \frac{\omega^2}{c^2}\mathbf{E}(\mathbf{r}) \\ \mathcal{L}_H\mathbf{H}(\mathbf{r}) &= \nabla\times[\frac{1}{\epsilon(\mathbf{r})}\nabla\times\mathbf{E}(\mathbf{r})] = \frac{\omega^2}{c^2}\mathbf{H}(\mathbf{r}) \end{aligned} \tag{7}$$

2.2 Photonic Eigenvalue Problem

Since the dielectric constant varies periodically in our medium, we can define lattice vectors $\{a_i\}$ with magnitudes equal to the periodicity of the dielectric constant.

$$\epsilon(\mathbf{r} + \mathbf{a_i}) = \epsilon(\mathbf{r}) \tag{8}$$

Because of this periodicity, we can expand $\epsilon^{-1}(\mathbf{r})$ in a Fourier series. For this, we introduce the elementary reciprocal lattice vectors $\{\mathbf{b_i}; 1, 2, 3\}$ and the reciprocal lattice vectors $\{\mathbf{G}\}$:

$$\begin{aligned} \mathbf{a_i}.\mathbf{b_j} &= 2\pi\delta_{ij} \\ \mathbf{G} &= l_1\mathbf{b_1} + l_2\mathbf{b_2} + l_3\mathbf{b_3} \end{aligned} \tag{9}$$

The inverse of the dielectric can then be expressed as,

$$\frac{1}{\epsilon(\mathbf{r})} = \Sigma_{\mathbf{G}}\kappa(\mathbf{G}) \exp\,[i\mathbf{G}.\mathbf{r}] \tag{10}$$

The solutions we seek for equation 2.7 are of the form,

$$\begin{aligned} \mathbf{E}(\mathbf{r}, t) &= \mathbf{E}(\mathbf{r})e^{i\omega t} \\ \mathbf{B}(\mathbf{r}, t) &= \mathbf{B}(\mathbf{r})e^{i\omega t} \end{aligned} \tag{11}$$

Since the dielectric constant is periodic in $\mathbf{r}$, we can apply Bloch's theorem to the spatial part of the electric and magnetic field solutions, analogous to the case of electronic states in a crystal. Hence we have,

$$\begin{aligned} \mathbf{E}(\mathbf{r}) = \mathbf{E}_{\mathbf{k}n}(\mathbf{r}) = \mathbf{u}_{\mathbf{k}n}(\mathbf{r})e^{i\mathbf{k}.\mathbf{r}} \\ \mathbf{H}(\mathbf{r}) = \mathbf{H}_{\mathbf{k}n}(\mathbf{r}) = \mathbf{v}_{\mathbf{k}n}(\mathbf{r})e^{i\mathbf{k}.\mathbf{r}} \end{aligned} \tag{12}$$

Here k is a wave vector in the first Brillouin zone and n is the band index. $\mathbf{u}_{\mathbf{k}n}(\mathbf{r})$ and $\mathbf{v}_{\mathbf{k}n}(\mathbf{r})$ are the periodic vectorial functions that satisfy the following relations,

$$\begin{aligned} \mathbf{u}_{\mathbf{k}n}(\mathbf{r} + \mathbf{a_i}) = \mathbf{u}_{\mathbf{k}n}(\mathbf{r}) \\ \mathbf{v}_{\mathbf{k}n}(\mathbf{r} + \mathbf{a_i}) = \mathbf{v}_{\mathbf{k}n}(\mathbf{r}) \end{aligned} \tag{13}$$

Since the electric and magnetic field solutions are periodic, they can be expanded into a Fourier series.

$$\begin{aligned} \mathbf{E}_{\mathbf{k}n}(\mathbf{r}) = \sum_{\mathbf{G}} \mathbf{E}_{\mathbf{k}n}(\mathbf{G}) \exp\,[i((\mathbf{k} + \mathbf{G}).\mathbf{r}] \\ \mathbf{H}_{\mathbf{k}n}(\mathbf{r}) = \sum_{\mathbf{G}} \mathbf{H}_{\mathbf{k}n}(\mathbf{G}) \exp\,[i((\mathbf{k} + \mathbf{G}).\mathbf{r}] \end{aligned} \tag{14}$$

Substituting the above form of the field solutions in equation 2.7, we have,

$$\begin{aligned} -\sum_{\mathbf{G}'} \kappa(\mathbf{G} - \mathbf{G}')(\mathbf{k} + \mathbf{G}') \times \{(\mathbf{k} + \mathbf{G}') \times \mathbf{E}_{\mathbf{k}n}(\mathbf{G}')\} = \frac{\omega_{\mathbf{k}n}^2}{c^2}\mathbf{E}_{\mathbf{k}n}(\mathbf{G}) \\ -\sum_{\mathbf{G}'} \kappa(\mathbf{G} - \mathbf{G}')(\mathbf{k} + \mathbf{G}') \times \{(\mathbf{k} + \mathbf{G}') \times \mathbf{H}_{\mathbf{k}n}(\mathbf{G}')\} = \frac{\omega_{\mathbf{k}n}^2}{c^2}\mathbf{H}_{\mathbf{k}n}(\mathbf{G}) \end{aligned} \tag{15}$$

Here, $\omega_{\mathbf{k}n}$ denotes the eigen-angular frequency of $\mathbf{E}_{\mathbf{k}n}$ and $\mathbf{H}_{\mathbf{k}n}$. By solving one of these two equations, we can obtain the dispersion relation of the eigenmodes, or the photonic band structure.

2.3 Numerical Methods for Photonic Band Structure and Transmission Spectra

For some photonic crystals, the solutions of Maxwell's equations can be obtained analytically. However, numerical methods must be employed to solve more complex problems. Here, we will be discussing about solving the problem in the frequency domain. One method is the plane-wave expansion method. In the plane wave expansion, the dielectric constant is approximated by a discrete Fourier series, and the electric/magnetic field is built out of plane waves. This method is used to solve for the eigenstates of Maxwell's eigenvalue problems (Eq. 15)

The transmission spectrum is numerically calculated using the finite-difference time-domain method(FDTD). FDTD is a time domain simulation method where space and time are divided into a grid of discrete points and the derivatives are approximated as finite differences. This method is generally used to calculate transmission and reflection spectra as it can compute the linear response of a system at multiple frequencies.

In this report, we have used the software package "MIT Photonic Bands"(MPB), and "MEEP". MPB is designed to compute definite-frequency eigenstates of Maxwell's equations in periodic dielectric structures. It is primarily used to study photonic crystals. "MEEP" is a Python package that is used to create FDTD simulations.

In the reference paper [8], the authors have used the package "MPB" to create simulations. This paper is the primary motivation of my thesis. In this paper, they have used Si/SiO_2 bilayers, but have tuned the thickness of the bilayers using the formula,

$$\begin{aligned} T_n &= T_0\{1 + Acos(2\pi\beta n)\} \\ \beta &= 144/89 \end{aligned} \tag{16}$$

Here, n corresponds to the n^{th} bilayer and β is the closest rational number to the diophantine number $\frac{1+\sqrt{5}}{2}$. Fig 1a shows the schematic of the sample used in the paper. Fig. 1c shows the plot of the photonic eigenvalue spectrum vs. the thickness parameter, along with the IPR values. Fig. 1b shows the comparison of the transmission spectrum obtained from the experiment and the numerical simulation.

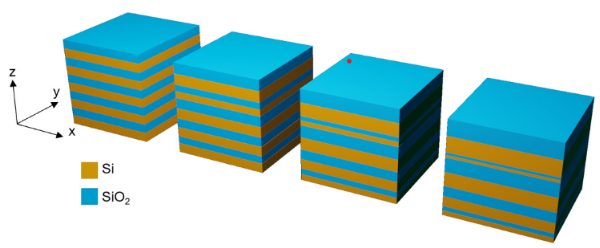

(a) Schematic of the sample used in reference paper.

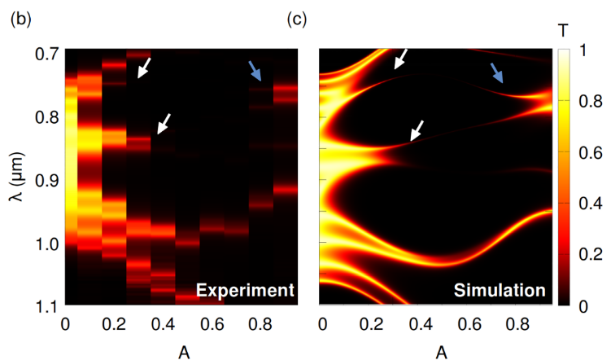

(b) Comparision of transmission spectrum from numerical simulation and experiment

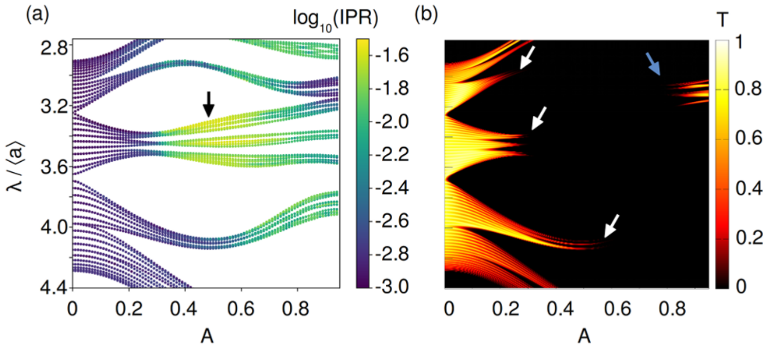

(c) The left image shows the eigenvalue spectrum and the IPR values as a function of the thickness parameter. The right image shows the plot of transmission plot vs the thickness parameter.

Figure 1: Cutouts from reference paper [8]

I was able to qualitatively replicate the eigenvalue spectrum without the IPR values (Fig. 2)

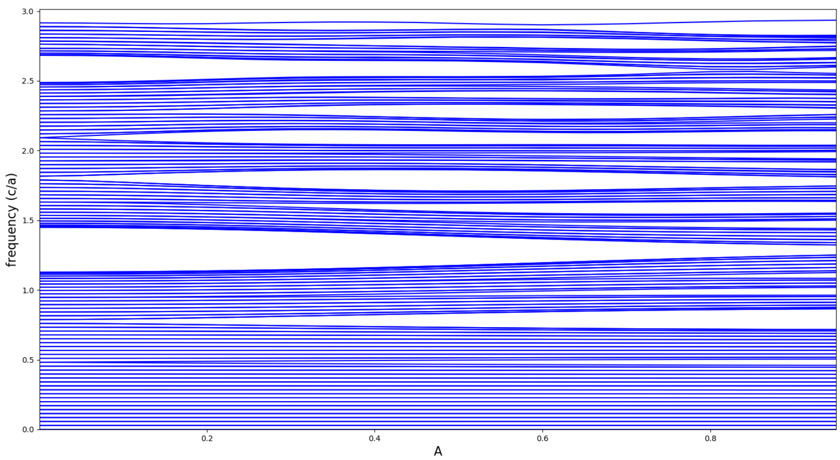

Figure 2: The eigenvalue spectrum as a function of thickness parameter of the same structure used in ref[8]

However, the IPR values that I calculated were not correct. I will try to solve this in the next semester.

For demonstration, a photonic crystal with structure ABAB is simulated. 3b shows the computational cell of the simulation. 3c and 3d shows the band structure and transmission spectrum, respectively, of a structure that closely resembles the dielectric multilayer used in the experiment.

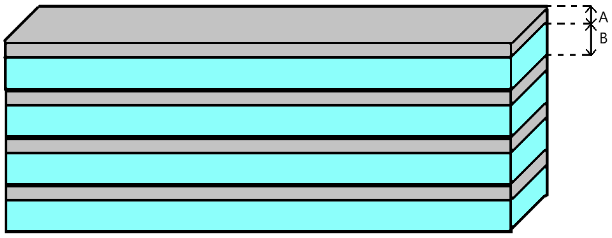

(a) Schematic of the sample used for simulation. A denotes the thickness of SiO_2, and B denotes the thickness of ZnO

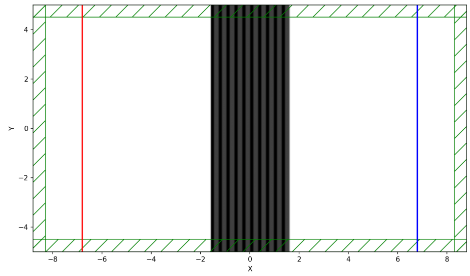

(b) Computational cell. The red line represents the source. The blue line represents the area where the flux is taken for calculating intensity.

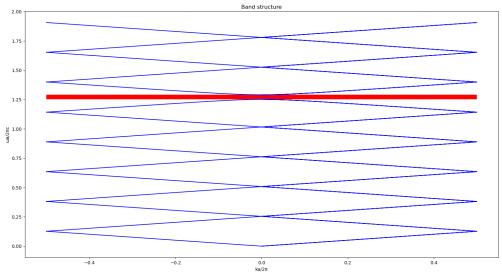

(c) Band structure of the simulated sample. The red shading indicates the bandgap.

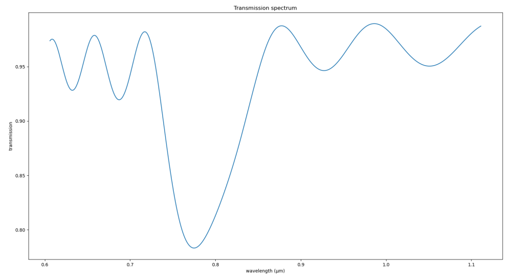

(d) Transimssion spectrum

Figure 3: Example of numerical simulation. The thickness of SiO_2 is taken to be 130 nm and that of ZnO is taken to be 190 nm.

3 Experimental methods and analysis

3.1 Sample fabrication

The 1-D photonic crystals are grown in the RF sputtering deposition system. The multilayer comprises ZnO(n = 1.6) and SiO_2(n = 1.45), deposited on a glass substrate. The sample consists of 10 bilayers, each composed of one layer of ZnO and one layer of SiO_2. The films are grown at room temperature. Argon gas was used for plasma inside the deposition chamber, and the deposition was done at a pressure of 3×10^{-2} mbar. The RF power was kept at 80W for both materials. Six silicon and six glass substrates were used to deposit the multi-layer. 4 shows the arrangement of the substrates on the substrate holder.

Figure 4: Substrate holder with all the substrates for depositing the multilayers.

The time of deposition for both layers of a single multilayer was kept the same (8 minutes). However, the thickness of the layer is not the same, as the amount of material deposited in a given time interval is different for different materials. This results in quasiperiodic photonic crystals of type ABAB, where A and B are the thickness of the ZnO and SiO2 in a single bilayer, respectively.

3.2 Characterization techniques

3.2.1 FESEM for surface morphology

The sample's surface was studied using FESEM. The operating voltage (EHT) was kept at 5 kV.

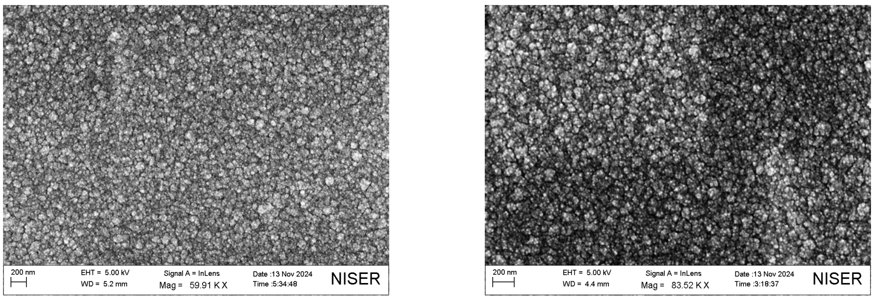

(a) (b)

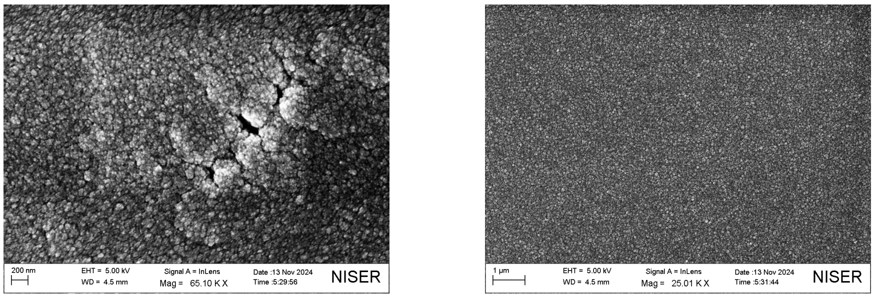

(c) (d)

Figure 5: SEM images of the sample surface. (a) and (b) are the images of the multilayer surface grown on a Silicon substrate. (c) and (d) are the images of the multilayer surface grown on the glass substrate.

The SEM images of the sample's surface are shown in 6. The surface is almost uniform except for some areas (5c), where there is a bit of non-uniform growth.

3.2.2 SEM-EDAX

The cross-section of the multilayer dielectric was studied in the FESEM setup. An EDAX measurement was conducted to map the components of a part of the entire cross-section containing the deposited layer and some layers of the substrate.

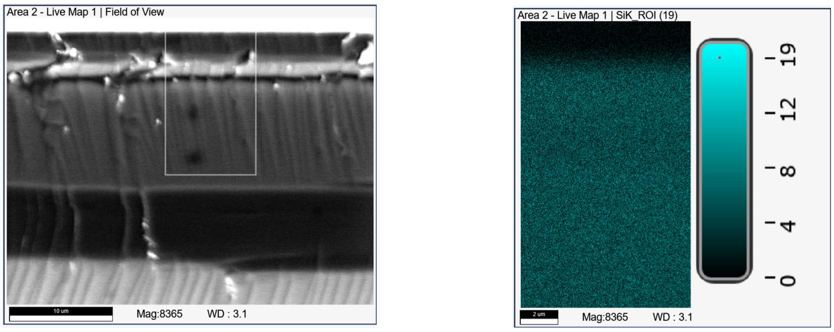

(a) (b)

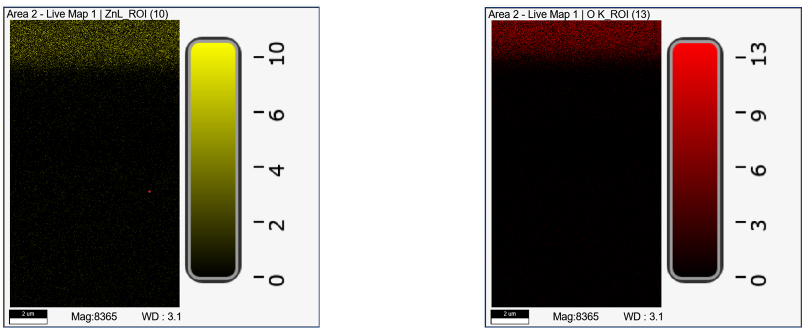

(c) (d)

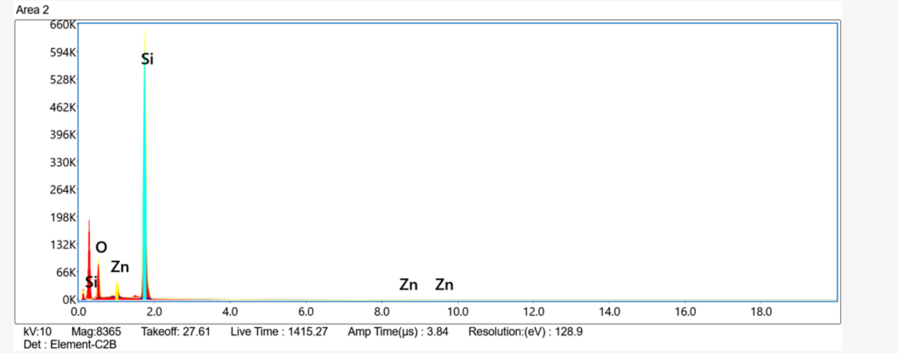

Element	Weight %	Atomic %	Error %	Net Int.
O K	13.20	21.80	7.70	396.70
Zn L	6.20	2.50	3.00	138.20
Si K	80.60	75.70	2.70	3710.80

(e)

Figure 6: EDAX measurements. a) An image of the cross-section. The white boundaries mark the region of interest. b) The map of Silicon in the region of interest. c) The map of Zinc in the region of interest. d) The map of Oxygen in the region of interest e) The plot of the number atoms vs energy

3.2.3 UV-Vis-NIR spectroscopy

The transmission spectra of the multilayers were measured in the Cary 5000 UV-Vis-NIR spectrophotometer. The wavelength range over which the transmittance was studied was from 250 nm to 2000 nm. 7 shows the setup for transmission spectrum measurement.

Figure 7: Setup for measuring transmission

The transmission spectrum of five samples was studied. The profile of the transmission spectrum for all the samples is similar, with slight variations in the transmittance values (8). We observe a significant decrease in the transmission values in the ultraviolet range (250-270 nm).

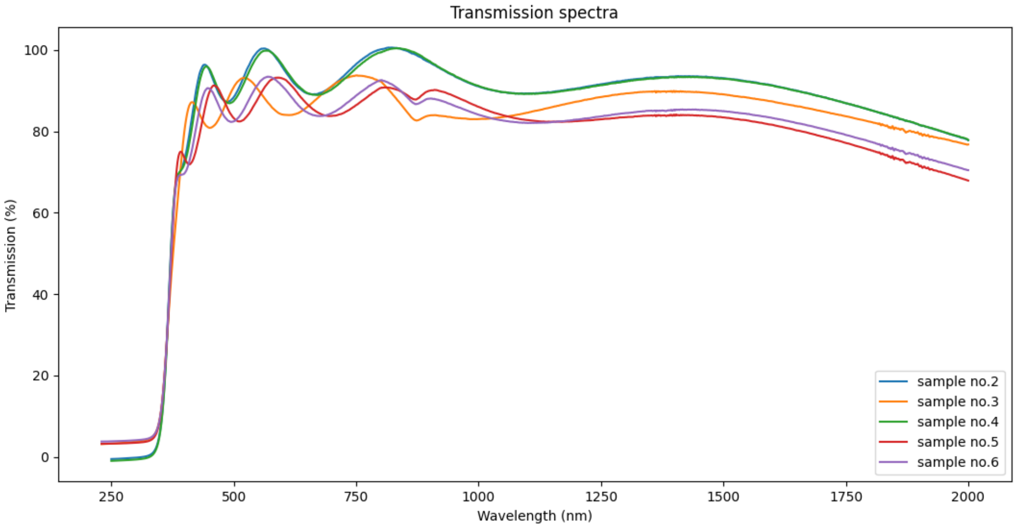

Figure 8: Transmission spectrum of the multilayer dielectric.

The decrease in the transmission values can be caused by the frequency of the incident light used within a photonic bandgap of the crystal. To verify this, we can plot the band structure of the multilayer and check for band gaps in the frequency range mentioned above. The transmission loss can also be attributed to the localization of the light modes. The extent of localization of a light mode can be calculated from its inverse participation ratio (IPR). Both of these quantities can be simulated numerically if the geometry of the photonic crystal is known to us.

4 Conclusion and Future Directions

In this project we explored the theoretical aspects of photonic crystals and photonic band structures. The numerical methods discussed will be helpful for correlating the band structure and transmission spectrum, which would explain the behavior of the transmission spectrum. We were able to create a 1-D photonic crystal using RF sputtering and studied its surface using SEM and EDAX. The transmission spectrum of the multilayer was measured using a UV-Vis-NIR spectrophotometer.

In order to get an idea about the thickness of the individual layers, a better characterization technique with better magnification and resolution has to be used, like TEM(Tunneling Electron Microscope). This is a part of the future studies. After the successful study of the multilayer, we will shift our attention to a quasiperiodic multilayer with more degree of aperiodicity, as given in [8].

References

[1] MEEP Developers. MEEP Documentation — meep.readthedocs.io. `https://meep.readthedocs.io/en/master/`. [Accessed 24-11-2024].

[2] MPB Developers. MPB Documentation — mpb.readthedocs.io. `https://mpb.readthedocs.io/en/latest/`. [Accessed 24-11-2024].

[3] Willy Dörfler, Armin Lechleiter, Michael Plum, Guido Schneider, and Christian Wieners. *Photonic Crystals: Mathematical Analysis and Numerical Approximation*. Springer Basel, Basel, 2011. URL: `https://link.springer.com/10.1007/978-3-0348-0113-3`, https://doi.org/10.1007/978-3-0348-0113-3 `doi:10.1007/978-3-0348-0113-3`.

[4] J. D. Joannopoulos, editor. *Photonic crystals: molding the flow of light*. Princeton University Press, Princeton, 2nd ed edition, 2008. OCLC: ocn180190957.

[5] Steven Johnson and John Joannopoulos. Block-iterative frequency-domain methods for Maxwell's equations in a planewave basis. *Optics Express*, 8(3):173, January 2001. URL: `https://opg.optica.org/oe/abstract.cfm?uri=oe-8-3-173`, https://doi.org/10.1364/OE.8.000173 `doi:10.1364/OE.8.000173`.

[6] Shilpi Roy, Tapan Mishra, B. Tanatar, and Saurabh Basu. Reentrant Localization Transition in a Quasiperiodic Chain. *Physical Review Letters*, 126(10):106803, March 2021. arXiv:2008.00489 [cond-mat]. URL: `http://arxiv.org/abs/2008.00489`, https://doi.org/10.1103/PhysRevLett.126.106803 `doi:10.1103/PhysRevLett.126.106803`.

[7] Kazuaki Sakoda. *Optical properties of photonic crystals: with 29 tables*. Number 80 in Springer series in optical sciences. Springer, Berlin Heidelberg, 2. edition edition, 2005.

[8] Sachin Vaidya, Christina Jörg, Kyle Linn, Megan Goh, and Mikael C. Rechtsman. Reentrant delocalization transition in one-dimensional photonic quasicrystals. *Physical Review Research*, 5(3):033170, September 2023. URL: `https://link.aps.org/doi/10.1103/PhysRevResearch.5.033170`, https://doi.org/10.1103/PhysRevResearch.5.033170 `doi:10.1103/PhysRevResearch.5.033170`.

[9] Da-Wei Yeh and Chien-Jang Wu. Analysis of photonic band structure in a one- dimensional photonic crystal containing single- negative materials. 2009.